Phytomedicine 85 (2021) 153546

Contents lists available at ScienceDirect

Phytomedicine

journal homepage: www.elsevier.com/locate/phymed

The triterpene, methyl-3β-hydroxylanosta-9,24-dien-21-oate (RA3), attenuates high glucose-induced oxidative damage and apoptosis by improving energy metabolism

Nonhlakanipho F. Sangweni [a,b], Rebamang A. Mosa [c], Phiwayinkosi V. Dludla [a,d], Abidemi P. Kappo [e], Andy R. Opoku [f], Christo J.F. Muller [a,b,f], Rabia Johnson [a,b,*]

[a] Biomedical Research and Innovation Platform (BRIP), South African Medical Research Council, Tygerberg 7505, South Africa
[b] Division of Medical Physiology, Faculty of Health Sciences, Stellenbosch University, Tygerberg 7505, South Africa
[c] Department of Biochemistry, Genetics and Microbiology (BGM), Division of Biochemistry, University of Pretoria, Hatfield 0028, South Africa
[d] Department of Life and Environmental Sciences, Polytechnic University of Marche, Ancona 60131, Italy
[e] Department of Biochemistry, Faculty of Science, University of Johannesburg, Auckland Park 2006, South Africa
[f] Department of Biochemistry and Microbiology, University of Zululand, KwaDlangezwa 3886, South Africa

ARTICLE INFO

Keywords:
Hyperglycemia
Triterpene
Oxidative stress
Diabetic cardiomyopathy
Apoptosis

ABSTRACT

Background: Hyperglycemia-induced cardiovascular dysfunction has been linked to oxidative stress and accelerated apoptosis in the diabetic myocardium. While there is currently no treatment for diabetic cardiomyopathy (DCM), studies suggest that the combinational use of anti-hyperglycemic agents and triterpenes could be effective in alleviating DCM.

Hypothesis: To investigate the therapeutic effect of methyl-3β-hydroxylanosta-9,24-dien-21-oate (RA3), in the absence or presence of the anti-diabetic drug, metformin (MET), against hyperglycemia-induced cardiac injury using an *in vitro* H9c2 cell model.

Methods: To mimic a hyperglycemic state, H9c2 cells were exposed to high glucose (HG, 33 mM) for 24 h. Thereafter, the cells were treated with RA3 (1 μM), MET (1 μM) and the combination of MET (1 μM) plus RA3 (1 μM) for 24 h, to assess the treatments therapeutic effect.

Results: Biochemical analysis revealed that RA3, with or without MET, improves glucose uptake via insulin-dependent (IRS-1/PI3K/Akt signaling) and independent (AMPK) pathways whilst ameliorating the activity of antioxidant enzymes in the H9c2 cells. Mechanistically, RA3 was able to alleviate HG-stimulated oxidative stress through the inhibition of reactive oxygen species (ROS) and lipid peroxidation as well as the reduced expression of the PKC/NF-κB cascade through decreased intracellular lipid content. Subsequently, RA3 was able to mitigate HG-induced apoptosis by decreasing the activity of caspase 3/7 and DNA fragmentation in the cardiomyoblasts.

Conclusion: RA3, in the absence or presence of MET, demonstrated potent therapeutic properties against hyperglycemia-mediated cardiac damage and could be a suitable candidate in the prevention of DCM.

Abbreviations: ADP, adenosine diphosphate; Akt, protein kinase B; AMPK, 5′ AMP-activated protein kinase; ANOVA, analysis of variance; ATP, adenosine triphosphate; BSA, bovine serum albumin; CAD, coronary artery disease; CVD, cardiovascular disease; DAGs, diacylglycerol; DCFH-DA, 2′-7′dichlorofluorescin diacetate; DCM, diabetic cardiomyopathy; DMEM, dulbecco's modified eagle medium; DMSO, dimethyl sulfoxide; DNA, deoxyribonucleic acid; DPBS, dulbecco's phosphate-buffered saline; FBS, fetal bovine serum; FFAs, free fatty acids; GLUT4, glucose transporter 4; GSH, reduced glutathione; GSSG, oxidized glutathione; HBSS, hanks balanced salt solution; HG, high glucose; IR, infrared; IRS-1, insulin receptor substrate 1; JC-1, 5,5′,6,6′-tetrachloro-1,1′,3,3-tetraethylbenzimidazolyl-carbocyanine iodide; MET, metformin; MMP, mitochondrial membrane potential; NF-κB, nuclear factor kappa B; NMR, nuclear magnetic resonance; ORO, oil red O; pent-strep, penicillin streptomycin; PI, propidium iodide; PI3K, phosphoinositide 3-kinases; PKC, protein kinase C; PMSF, phenylmethylsulfonyl fluoride; RA3, methyl-3β-hydroxylanosta-9,24-dien-21-oate; ROS, reactive oxygen species; SOD, superoxide dismutase; T2DM, type 2 diabetes mellitus; TBARS, thiobarbituric acid reactive substances; TdT, terminal deoxynucleotidyl transferase; Tris/HCl, trizma/hydrochloride.

* Corresponding author.
E-mail addresses: nonhlakanipho.sangweni@mrc.ac.za (N.F. Sangweni), phiwayinkosi.dludla@mrc.ac.za (P.V. Dludla), christo.muller@mrc.ac.za (C.J.F. Muller), rabia.johnson@mrc.ac.za (R. Johnson).

https://doi.org/10.1016/j.phymed.2021.153546
Received 23 August 2020; Received in revised form 11 February 2021; Accepted 5 March 2021
Available online 10 March 2021

Introduction

Diabetic cardiomyopathy (DCM) is defined as the existence of abnormal cardiac structure and performance in the absence of other cardiovascular disease (CVD) risk factors in individuals with diabetes (Jia et al., 2018). Such individuals, especially those presenting with type 2 diabetes mellitus (T2DM) are characterized by dyslipidaemia, hyperglycemia and hyperinsulinemia; the important abnormalities implicated in the development of DCM (Borghetti et al., 2018). Generally, coronary artery disease (CAD) is regarded as the most prominent CVD in both diabetic and non-diabetic individuals (Hajar et al., 2017) however, the discrepancy pertaining to the development and progression of cardiovascular abnormalities in those with diabetes could explain the "low prevalence" of DCM. Also, patients that develop DCM may also present with CAD as the disease progresses (Marcinkiewicz et al., 2017), which corroborate why DCM remains poorly diagnosed. Although first described nearly four decades ago (Rubler et al., 1972), the pathophysiology underlying the distinctive mechanism of DCM remains poorly understood.

Over the years, multiple metabolic abnormalities including impaired lipid and glucose metabolism, mitochondrial dysfunction, oxidative stress, inflammation and loss in metabolic flexibility (Isfort et al., 2014; Tate et al., 2017; De Rosa et al., 2018) have all been implicated in the physiopathology of DCM. Generally, in order to meet its high energy demands, the adult heart uses multiple substrates to generate ATP production, a phenomenon called "metabolic substrate flexibility" (Borghetti et al., 2018). Here, free fatty acids (FFAs) are the preferred energy substrate trailed by glucose. However, the diabetic heart which often presents with prolonged hyperglycemia and insulin resistance may result in a complete loss of metabolic flexibility. During this state, the decrease in glucose metabolism stemming from enhanced supply of FFAs forces a complete reliant on β-oxidation with a concomitant increase in the accumulation of lipids in the cardiomyocytes (Borghetti et al., 2018). This switch in energy metabolism and abnormal lipid storage is accompanied by the increased generation of reactive oxygen species (ROS) and impaired oxidative phosphorylation, which stimulates mitochondria depolarization thereby, causing a loss in cardiac efficiency (Bugger and Abel, 2010; Rider et al., 2013. Subsequently, the diabetic heart is left susceptible to oxidative stress, aggravated apoptosis and pathological remodelling (Zhao et al., 2017; Jia et al., 2018).

Although several hypoglycemic agents, such as metformin, are targeted to effectively regulate blood glucose levels and possibly limit the risk of DCM, there remains a lack of specific treatment to protect against hyperglycemia-induced cardiac damage (Tate et al., 2017). Furthermore, it is speculated that recent advances, particularly in the area of alternative medicine as a co-treatment to current diabetic drugs such as metformin (Gawli and Lakshmidevi, 2015; Dludla et al., 2018), may prove effective in protecting against diabetes and its associated cardiovascular complications (Tate et al., 2017). Thus, there is an increasing interest in understanding the biological properties of plant-derived compounds for their ameliorative effects against diabetes and its associated complications. Accordingly, several polyphenolic compounds have been reported to effectively alleviate the burden of diabetes related cardiovascular complications when used in combination with anti-diabetic drugs (Naruszewicz et al., 2007; Johnson et al., 2016; Rahimi et al., 2021) Consistent with this interest, our group has progressively demonstrated the beneficial effects of triterpenes isolated from *Protorhus longifolia* (Bernh) Engl. against diabetes-associated complications in various experimental models, as recently reviewed by Sangweni and colleagues (2018). A prime example is the lanostane type of triterpene, methyl-3β-hydroxylanosta-9, 24-dien-21-oate (RA3) that has demonstrated promising anti-hyperglycemic properties (Mosa et al., 2015). The hypoglycemic effect, of the triterpene has been linked its capacity to improve glucose tolerance by mediating the insulin transduction pathway in streptozotocin-induced diabetic rats (Mosa et al., 2015, Mabhida et al., 2018). More precisely, evidence shows that RA3 can improve insulin signalling by effectively regulating the insulin-receptor substrate 1/ phosphoinositide 3-kinase/ protein kinase B (IRS-1/PI3K/Akt) protein pathway, while also increasing antioxidant defence and mitigating lipid peroxidation in experimental models of diabetes (Mosa et al., 2015, Mabhida et al., 2018)

Relevant to the heart, RA3 has been shown to reduce myocardial fat deposition whilst improving intracellular antioxidant enzyme activity in high-fat diet fed rats (Mosa et al., 2016)]. Since cardiomyocytes are not specialized to store lipids, these findings suggest that RA3 could possess therapeutic properties necessary to aid in alleviating DCM. Accordingly, in this study, we aimed to investigate whether RA3 could protect cardiomyoblasts against high glucose-induced damage. With the specific focus being the assessment of the therapeutic effects of this triterpene in correcting markers involved in cardiac substrate metabolism, oxidative stress and inflammation, which are the prominent pathological mechanisms implicated in DCM.

Materials and methods

Reagents

Dulbecco's Modified Eagle Medium (DMEM), Fetal Bovine Serum (FBS), Bovine serum albumin (BSA), Penicillin Streptomycin (pen-strep), tissue culture grade water, dimethyl sulfoxide (DMSO), Dulbecco's phosphate-buffered saline (DPBS), trypsin, Hanks balanced salt solution (HBSS), Bovine serum albumin (BSA) and ViaLight plus ATP kit were obtained from Lonza Walkersville, MD, USA. metformin, 5,5′,6,6′-tetrachloro-1,1′,3,3-tetraethylbenzimidazolyl-carbocyanine iodide (JC-1), phenylmethylsulfonyl fluoride (PMSF), trizma/hydrochloride (Tris/HCl), propidium iodide (PI), chloroform and glucose transporter 4 (GLUT4) were obtained from Sigma-Aldrich, St Louis, MO, USA. Sodium hydroxide (NaOH) and sodium dodecyl sulfate solution were purchased from Merck, Whitehouse Station, NJ, USA. Annexin V, fluorescein conjugate (FITC annexin V) was purchased from Invitrogen, Carlsbad, CA, USA. The thiobarbituric acid reactive substance (TBARS) kit and oxiselect™ intracellular ROS Assay Kit (Green Fluorescence) were obtained from Cell Biolabs, San Diego, USA. Superoxide dismutase (SOD) and β-methylphenethylamine (β-ME) was obtained from Abcam, Cambridge, United Kingdom. Glutathione (GSH), caspase-glo 3/7 and DeadEnd Fluorometric TUNEL kit were purchased from Promega, Madison, Wilsconsin, USA. Phosphorylated 5′ AMP-activated protein kinase (AMPK) at Thr172, phosphorylated nuclear factor kappa-light-chain-enhancer of activated B cells (NF-κβ) at Ser536, phosphorylated protein kinase C (PKC) at Ser660, phosphorylated IRS-1 at Ser307 and phosphorylated Akt-B at Thr308 were purchased from Cell signalling, Danvers, MA, USA. Anti-β actin was purchased from Santa Cruz Biotechnology, Santa Cruz, CA, USA.

Isolation and confirmation of methyl-3β-hydroxylanosta-9, 24-dien-21-oate (RA3)

The plant extract was prepared from the fresh stem bark of P. longifolia which was collected from KwaZulu-Natal, South Africa. Identity of the plant material with voucher specimen number RA01UZ was confirmed by a botanist at the University of Zululand. The targeted compound, methyl-3β-hydroxylanosta-9, 24-dien-21-oate (RA-3) (Fig. 1) was routinely isolated and purified from the chloroform extract of the plant material, using the method well described by (Mosa et al., 2014). The lanosteryl triterpene was isolated over silica gel chromatography and the isolated compound was recrystallized in ethyl acetate (100%) to obtain a pure compound (> 95% purity). Melting point and spectroscopic (IR, NMR) data analysis were used, in comparison with literature data (Mosa et al., 2014, Machaba et al., 2014) to confirm the chemical structure of the isolated lanosteryl triterpene. The physical (white crystals, melting point 204–205 °C) and spectral data of this compound were all in agreement with previous reports from our

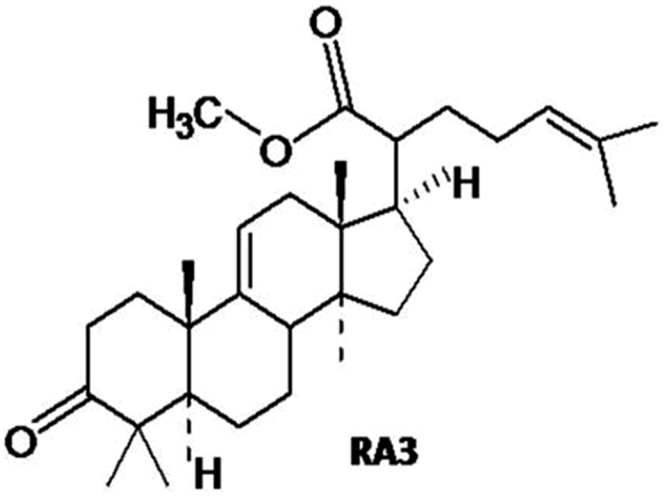

Fig. 1. Chemical structure of methyl-3β-hydroxylanosta-9, 24dienoate (RA3).

laboratory (Mosa et al., 2014, Machaba et al., 2014).

Cell culture conditions

Embryonic rat heart derived H9c2 cardiomyoblasts were acquired from the European Collection of Cell Cultures (ECACC No. 8809294) and used to carry out all experimental procedures. The cells were cultured in DMEM, supplemented with 10% FBS and 1% Pen-Strep, until they reached 80–90% sub-confluence under typical tissue culture conditions (TC- 37 °C, 95% humidified air and 5% CO_2). Experiments carried out in the present study were conducted with H9c2 cells at passages ranging from 21–26. Cells seeded in either 6-well, 24-well or 96-well plates, depending on the experiment performed, were washed with DPBS and then exposed to 33 mM high glucose (HG) treatment media (DMEM (without phenol red) supplemented with 1% BSA) for 24 h, in order to mimic a hyperglycemic state. This is an accomplished model to study complications associated with DCM *in vitro*, as previously reported by our group and others (Johnson et al., 2016; Davargaon et al., 2018). Cells exposed to low glucose (NG- 5.5 mM) served as the normal experimental control. The biochemical parameters measured in the current study were adopted from a recent study performed in our laboratory (Johnson et al., 2019).

Treatment preparation

Briefly, RA3 (MW: 470.74 g/mol) at 32 mg, was dissolved in 100 µl DMSO (100%) to yield an initial stock solution of 679.7 mM. To dilute the DMSO concentration, a final stock solution of 1 mM was prepared by diluting 7.4 µl of the initial stock with 5 mL DMEM (without phenol red, supplemented with 0.1% BSA). Thereafter, a final working concentration of 1 µM, with a DMSO concentration less than 0.001%, was prepared by pipetting 10 µl of the working solution to 10 ml of either 5.5 mM or 33 mM glucose treatment media. Furthermore, to assess the therapeutic effects of RA3 to ameliorate high glucose-induced cardiac stress, H9c2 cells were treated with either RA3 or metformin, as a monotherapy or combination, at 1 µM for 24 h. Cells exposed to normal glucose served as experimental controls, while metformin was employed as a comparative drug, as previously executed (Johnson et al., 2016).

Glucose uptake

Intracellular glucose uptake was measured according to the methods previously described by Johnson et al. (2016). High glucose-stimulated cells were probed with a radiolabeled glucose analog, 2-Deoxy-[3H]-D-glucose (DOG), before being lysed with a sodium hydroxide and sodium dodecyl sulfate solution. Ten microliters of the cell lysate was used for protein concentration analysis using the Bio-Rad DC Protein Assay. Thereafter, the cell lysates were transferred into scintillation vials containing 1 ml TC grade H_2O which was followed by the addition of a scintillation fluid (8 ml of Ready Gel Ultima Gold) and overnight equilibration and RT. Glucose uptake was determined in a liquid scintillation analyzer (2200 CA, Parkard Tricarb series) by liquid scintillation (PerkinElmer, Downers, Crove, IL, USA). The results were calculated using a counts and disintegration per minute (CPM; DPM) program:

(http://www.graphpad.com/quickcalcs/radcalcform.cfm). Protein concentrations and CPM were used to determine the fmol/mg.

Intracellular lipid content determination

Lipid storage in H9c2 cardiomyoblasts was assessed using an Oil-Red O (ORO) staining technique adapted from Sanderson *et al.* (2014). Briefly, treated cells were stained with 0.7% (v/v) ORO (made by diluting 1% stock (w/v) in TC grade water) and incubated for 30 min at room temperature before reading absorbance at 570 nm using the Bio-Tek® ELX800 plate reader (Gen5™ software). Subsequently, cells were counterstained with 0.5% crystal violet and absorbance read at 490 nm using the BioTek® ELX800 plate reader (Gen5™ software) in order to compensate for cell density. Intracellular lipid content was normalized to cell density as measured with crystal violet.

Expression of insulin-dependent and independent proteins

Protein expression, in high glucose-stimulated H9c2 cells, was quantified using Western blot analysis as previously described (Johnson et al., 2019). The following primary antibodies were used to quantify the expression of proteins involved in insulin signalling and energy homeostasis: p-AMPK(Thr172) (1:800), p-NF-κB (1:1000), GLUT4 (1:1000), p-IRS (Ser307) (1: 1000), p-PKC (Ser660) (1: 1000) and p-Akt (Thr308) (1: 500). β-actin (1:4000) was used as a housekeeping protein and a means to normalize the targeted proteins. Protein detection was performed using the enhanced chemiluminescence kit on the ChemiDoc XRS System (Bio-rad, USA). The band densities were analysed using the Image J software.

Quantification of prooxidants and antioxidants

The levels of superoxide dismutase (SOD) were measured using an Abcam SOD activity kit as per manufacturer's instructions (details of company). Absorbance was read at 450 nm with a BioTek® ELX800 plate reader (Gen5® software). Total GSH content was assessed using a GSH/GSSH-Glo™ assay kit, as previously described by Shabalala and colleagues (2019). Luminescence was assessed by a BioTek® FLX 800 plate reader using Gen5® software. Intracellular production of ROS was evaluated by exposing cardiomyoblasts to 100 µl of 2′, 7"-dichlorfluoresceindiacetatefluorescent dye (DCFH-DA- 1 µM, made up in HBSS fluorescent dye) and incubated under standard TC conditions for 30 min. Thereafter, the dye was eluted by the addition of HBSS which was followed by measuring DCFH-DA fluorescent intensity (emission spectra of 528 ± 20 nm) by means of a BioTek® FLx800 plate reader. Lipid peroxidation was quantified with an OxiSelect™ thiobarbituric acid reactive substances (TBARS) assay Kit (Cell Biolabs, San Diego, US), as per the instructions of the manufacturer using a BioTek® ELX800 plate reader (Gen5® software).

Determining changes in mitochondrial membrane potential and ATP activity

High glucose-stimulated depolarized mitochondria were evaluated by subjecting H9c2 cells to 5,5′,6,6′-tetrachloro-1,1′,3,3-

tetraethylbenzimidazolyl-carbocyanine iodide (JC-1) cationic dye. Briefly, treated cells were stained with 2 μM of JC-1 solution and thereafter, incubated in the dark for 30 min under standard TC conditions. Subsequently, the fluorescent intensity of JC-1 was assessed by measuring fluorescence at a single excitation 485 ± 20 nm; and dual emission 530 ± 25 nm and 590 ± 35 nm) in a BioTek® FLx800 plate reader. ATP as a measurement of metabolic activity was quantified using the ViaLight plus ATP kit (Lonza, Walkersville, MD, USA), as per the manufacturer's guidelines. Luminescence was measured on the SpectraMax i3x®Multi-Mode Microplate Reader.

TUNEL assay

DNA fragmentation was assessed by means of a DeadEnd Fluorometric TUNEL kit (Promega, Madison, Wilsconsin, USA), as per the manufacturer's instructions. Cells were stained with terminal deoxynucleotidyl transferase (TdT) reaction mixture and then incubated under standard TC conditions for 60 min. The rate of DNA fragmentation was quantified as the mean of condensed TUNEL-positive cells, as shown by green fluorescence, in non-overlapping fields of 1 mm^2 under 10 × magnification field (average of at least 5 fields per well). Data was normalized against the DAPI staining, which was indicated as blue fluorescence. Fluorescence was measured with a Nikon Eclipse Ti inverted fluorescence microscope equipped with a NIS Elements imaging software.

Annexin V and propidium iodide assays, and caspase 3/7 activity

Annexin V-FITC (Invitrogen, Carlsbad, CA, USA) and propidium iodide (PI, Sigma-Aldrich, St Louis, MO, USA) were used to quantify early and late apoptosis in the H9c2 cells. Briefly, cells were stained with 0.5% of annexin v and 1 μg/ml of PI and then incubated for 30 min. Thereafter, fluorescence was measured on the SpectraMax i3x®Multi-Mode Microplate Reader at an emission spectra of 485 ± 20/ 528 ± 20 nm, for annexin V, and 530 ± 25/ 590 ± 35 nm, for PI. Additionally, the activity of caspase 3/7 was measured using the Caspase-Glo® 3/7 luminescent assay kit (Promega Corporation) as per the manufacturer's instructions. Luminescence was measured using the SpectraMax i3x®Multi-Mode Microplate Reader and then normalized to protein concentrations.

Statistical analysis

All data were statistically analysed using GraphPad Prism software version 5.0 (GraphPad Software, Inc. La Jolla, USA). The data are represented as the mean ± standard error of mean (SEM) of three independent biological experiments, with each experiment containing at least six replicates. Comparisons between treatment groups were performed using one-way analysis of variance (ANOVA), followed by a Tukey post hoc test and a student's *t*-test. A *p*-value $\leq$ 0.05 was considered as statistically significant.

Results

RA3; In the presence or absence of MET; Improves glucose uptake whilst reducing lipid storage

Impaired substrate preference is a prominent abnormality associated with the pathogenesis of DCM. As such, the effect of RA3 on intracellular glucose uptake and lipid accumulation was investigated. The results demonstrated that high glucose (HG) exposure significantly decreases glucose uptake ((51.75 ± 6.77%, $p \leq 0.01$) (Fig. 2A) through the apparent increase in intracellular lipid content (265.50 ± 7.15%; $p \leq 0.001$) in the H9c2 cells (Fig. 2B). However, upon treatment with RA3, impaired substrate preference was noticeably reduced in these cells as demonstrated by improved glucose uptake (75.75 ± 6.33%, $p \leq 0.05$) and reduced lipid content (100.3 ± 5.57%; $p \leq 0.001$). Likewise, a comparable effect was observed in substrate metabolism in cells treated with MET (88.42 ± 12.56%; $p \leq 0.01$ and 89.75 ± 6.06; $p \leq 0.001$). Interestingly, a synergistic improvement in cellular glucose uptake (171.4 ± 30.31%; $p \leq 0.001$) was observed in cardiomyoblasts co-treated with MET plus RA3 when compared to cells treated with either RA3 or MET alone (Fig. 2A).

Effect of RA3 and MET on glucose metabolism

The effect of hyperglycemia on the myocardium reportedly stimulates the phosphorylation of NF-κB through the diacylglycerol-PKC signal transduction pathway, which is a central aspect of insulin resistance and resultant cardiac injury. Here, PKC expression was significantly increased (18630 ± 862.3; $p \leq 0.001$) by HG exposure which led to the accelerated activation of NF-κB (525.4 ± 25.5; $p \leq 0.001$) in these cells (Fig. 3A and B). As a result, a considerable reduction in glucose

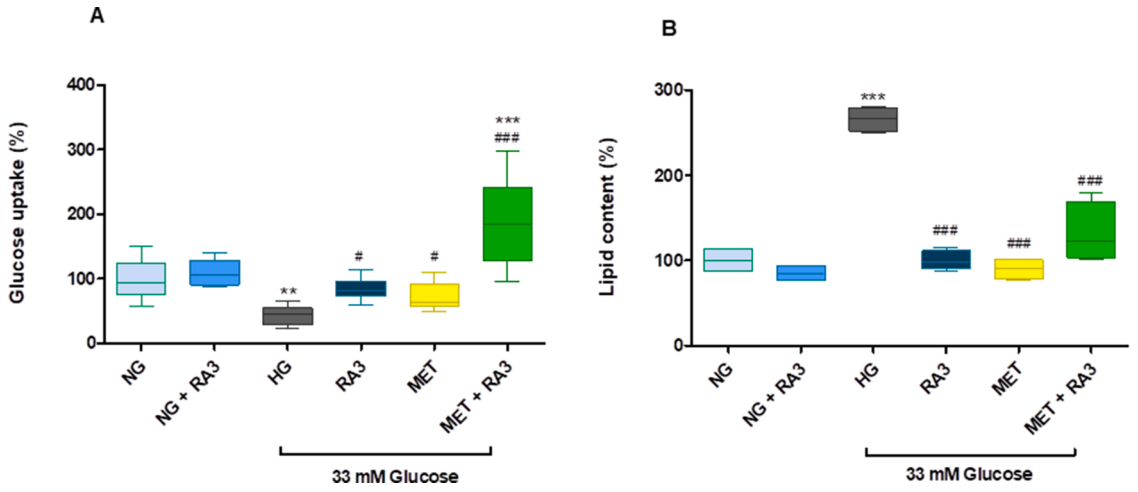

Fig. 2. The effect of methyl-3β-hydroxylanosta-9, 24-dienoate (RA3) and metformin (MET) on glucose uptake and lipid accumulation. (A) Glucose uptake and (B) lipid content in high glucose (HG, 33 M) stimulated H9c2 cardiomyoblasts. Cells exposed to HG were treated with RA3 (1 μM), MET (1 μM) and a combination of MET+RA3 (both at 1 μM). Cells exposed to normal glucose (NG, 5.5 mM) served as the normal control. Data are presented as the mean ± SEM of 3 distinct biological experiments with each experiment having 3 practical repeats (n = 3). Significance is depicted as ** $p \leq 0.01$, *** $p \leq 0.001$ *vs.* NG control, $^{\#}$ $p \leq 0.05$, $^{\#\#\#}$ $p \leq 0.001$ *vs.* HG control.

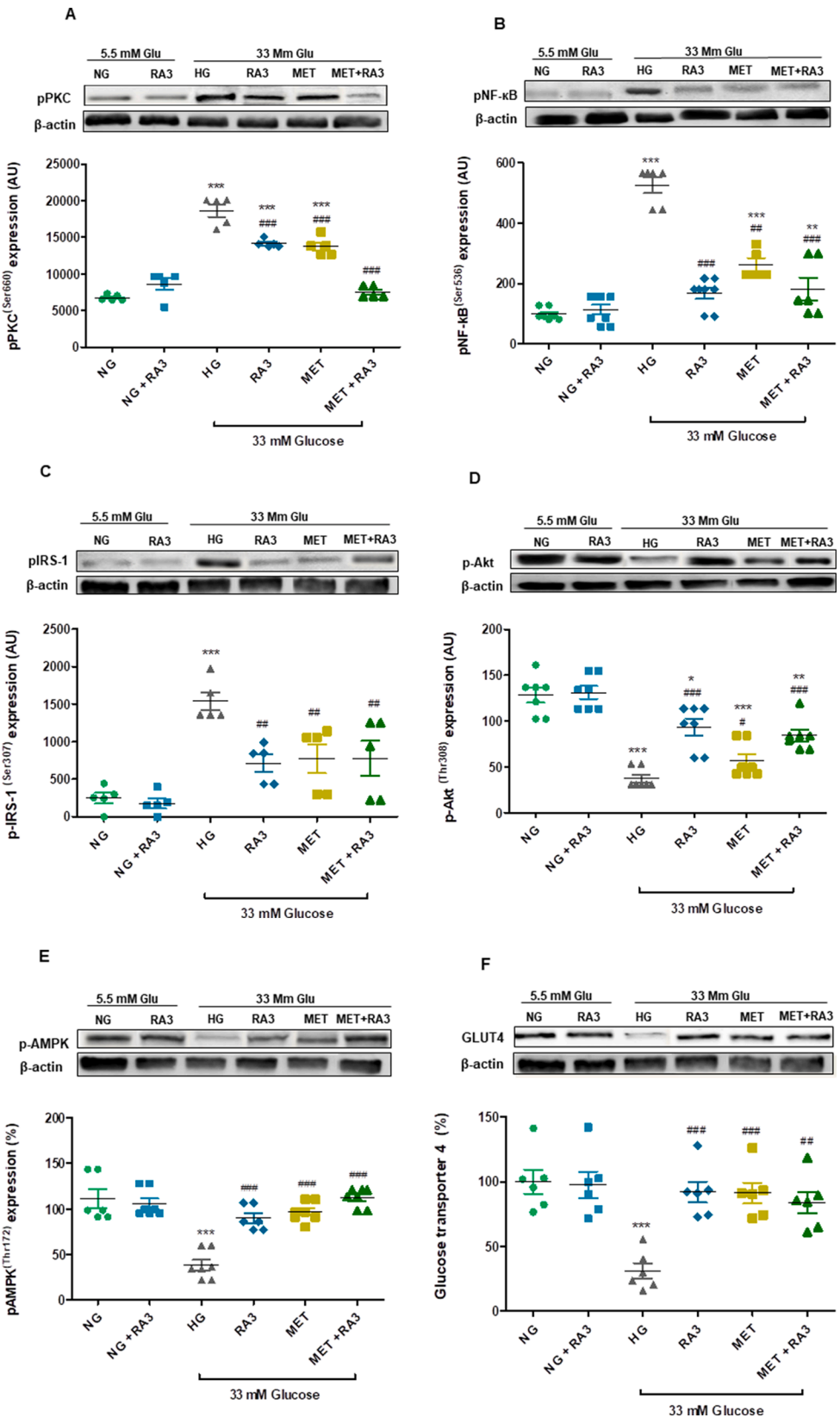

Fig. 3. Methyl-3β-hydroxylanosta-9, 24-dienoate (RA3), in the presence or absence of metformin (MET), ameliorates glucose metabolism. The following proteins were quantified: (A) protein kinase C (PKC), (B) nuclear factor kappa beta (NF-κB) (PKC), (C) insulin receptor substrate-1 (IRS-1), (D) protein kinase B (Akt). (E) 5′ adenosine monophosphate-activated protein kinase (AMPK) and (E) glucose transporter 4 (GLUT4) in high glucose (Glu) stimulated H9c2 cells. Results are expressed as the mean ± SEM of 3 independent biological experiments with each experiment having 3 technical replicates (n = 3). Significance is depicted as * $p \leq 0.05$, ** $p \leq 0.01$, *** $p \leq 0.001$ *vs.* NG control, $^{\#}$ $p \leq 0.05$, $^{\#\#}$ $p \leq 0.01$, $^{\#\#\#}$ $p \leq 0.001$ *vs.* HG control.

metabolism through activated serine phosphorylation of IRS-1 (1538 ± 122.0; $p \leq 0.001$), which impairs insulin signalling, was observed (Fig. 3C). Although cardiomyoblasts treated with RA3 (14126 ± 242.8; $p \leq 0.001$) and MET (13744 ± 557.5; $p \leq 0.001$) presented with decreased PKC expression, a significantly higher reduction was observed through co-treatment with MET plus RA3 (7508 ± 349.7; $p \leq 0.001$). Similarly, the phosphorylation of NF-κB (166.7 ± 17.4; $p \leq 0.001$) and IRS-1 (711.5 ± 115.5; $p \leq 0.01$) were noticeably decreased by RA3 treatment thereby, improving insulin sensitivity. Consequently, the rate of glucose metabolism was significantly ameliorated via the enhanced

expression of insulin dependent and independent proteins Akt (93.6 ± 9.1%; $p \leq 0.001$) and AMPK (89.9 ± 5.5%; $p \leq 0.001$), which collectively increased the cytosolic translocation of GLUT4 (91.9 ± 8.1%; $p \leq 0.001$) to the plasma membrane (Fig. 3D, E and F). Likewise, improved glucose transport was also observed in cells treated with MET ($p \leq 0.001$) and co-treated with MET plus RA3 ($p \leq 0.001$).

Effect of RA3 and MET on oxidative stress

Hyperglycemia-induced oxidative stress, as measured by ROS activity and lipid peroxidation, is a key component in the development of DCM. In this study, a significant increase in the production of ROS ($p \leq 0.01$) and MDA ($p \leq 0.001$) were observed in HG-stimulated cells when compared to the normal control. These findings were corroborated by the significant reduction in antioxidant enzyme activity in cells exposed to HG ($p \leq 0.05$). However, HG-induced oxidative stress was noticeably mitigated when cell were treated with RA3 ($p \leq 0.001$), MET ($p \leq 0.001$) or the combination of MET plus RA3 ($p \leq 0.001$), as demonstrated by the significant increase in GSH content and SOD activity (Table 1). Evidently, the improved activity of endogenous antioxidants in RA3 treated cells presented with reduced ROS and MDA content. Interestingly, a slightly more enhanced improvement in SOD ($p \leq 0.001$) and GSH ($p \leq 0.001$) activity was demonstrated by cells co-treated with MET plus RA3 when compared to those treated with MET alone, suggesting that RA3 might have an additive effect on MET (Table 1).

Effect of RA3 and MET on mitochondrial membrane potential (MMP) and metabolic activity

Altered cardiac mitochondrial function and resultant loss in metabolic activity are said to be amongst the underlying mechanisms of DCM. In the present study, a significant increase in the ratio of monomers vs. J-aggregates was observed in HG-stimulated cells (3.1 ± 0.2; $p \leq 0.001$), suggesting an increase in mitochondrial depolarization (Fig. 4A). Consequently, a loss in mitochondrial function which was demonstrated by the apparent reduction in cellular metabolic activity was observed in the HG-stimulated cells (46.0 ± 4.3%; $p \leq 0.001$) (Fig. 4B). Nonetheless, treatment with RA3 ($p \leq 0.001$), MET ($p \leq 0.001$) and the combination of MET plus RA3 ($p \leq 0.001$) proved to be considerably effective in mitigating HG-induced mitochondrial depolarization and thus, improved mitochondrial function. Interestingly, a synergistic improvement in cellular metabolic activity was observed when cells were co-treated with MET plus RA3 (146.1 ± 28.9%; $p \leq 0.001$). This improvement was noticeably much higher than the metabolic activity measured in the control ($p \leq 0.05$) (Fig. 4A and B).

Effect of RA3 and MET on DNA fragmentation

Diabetic patients are highly susceptible to oxidative DNA damage with a significantly higher frequency reported in DCM. In line with previous reports, our data demonstrated a considerably increased degree of fragmented DNA in H9c2 cells exposed to HG when compared to the control group (12.6 ± 2.0 compared to 1.8 ± 0.8, $p \leq 0.001$). However, treatment with RA3 (5.9 ± 1.1, $p \leq 0.01$) and MET (6.5 ± 2.0, $p \leq 0.05$) was able to significantly reduce the rate of nuclear DNA fragmentation in these cells. This reduction might have been attributed to RA3's ability to increase the levels of endogenous antioxidants. Additionally, RA3 appeared to have an additive effect on the efficacy of MET (6.5 ± 2.0, $p \leq 0.05$) as demonstrated by the much higher improvement in intact DNA observed in cells co-treated with MET plus RA3 (4.5 ± 0.7, $p \leq 0.01$) (Fig. 5A and B).

Effect of RA3 and MET on the rate of apoptosis

Cell death, as a comprehensive consequence of myocardial abnormalities, is a fundamental aspect of DCM. The rate of apoptosis was significantly accelerated by HG glucose exposure as demonstrated by an increase in cells going into early (140.4 ± 12.8%; $p \leq 0.001$) and late apoptosis (148.5 ± 10.9%; $p \leq 0.001$). These findings were confirmed by the increased activity of caspase 3/7 in these HG-stimulated cells (205.4 ± 5.1%; $p \leq 0.001$). Conversely, RA3 further demonstrated its cardioprotective potential through its apparent reduction of caspase 3/7 activation (162.9 ± 6.6%; $p \leq 0.001$), which led to a significant decrease in the degree of apoptosis ($p \leq 0.001$) (Fig. 6A, B and C). Likewise, cells treated with MET ($p \leq 0.01$) as well as the combination of MET plus RA3 ($p \leq 0.001$) also presented with a noticeable reduction in HG-induced apoptosis.

Discussion

The current study investigated the protective effects of RA3 or its combination with metformin in ameliorating high glucose-induced myocardial impairments *in vitro*. The high-glucose exposed H9c2 cardiomyoblasts represent an established *in vitro* model to study complications associated with the development of DCM (Luo et al., 2014; Sun et al., 2017; Zhang et al., 2018). Similar to diabetic patients, exposure of these cells to elevated glucose concentrations has been linked with the development of insulin resistance, a state mainly driven by impaired myocardial substrate metabolism. For example, in diabetic individuals, the prolonged effects of hyperglycemia is associated with insulin resistance and increased availability of FFAs, a process that suppresses glucose uptake (Ormazabal et al., 2018; Makarova et al., 2019). Similarly, results from the current study demonstrated that exposure of these cardiac cells to hyperglycemic conditions was consistent with the suppression of glucose uptake and ATP production. Although not assessed in the current study, suppression of glucose uptake has been reported to be concomitant with abnormally increased FFA oxidation (Johnson et al., 2016). To verify the insulin-resistant state, the current findings revealed that in addition to impaired substrate metabolism, high glucose exposure was responsible for increased NF-κB phosphorylation, a redox-sensitive transcription factor essential for regulating a number of inflammatory genes. More importantly, inhibition of NF-κB, together with PKC has been a plausible strategy to manage CVD-related complications (Wang et al., 2009; Suryavanshi and Kulkarni, 2017). Interestingly, both NF-κB and PKC have been ideal therapeutic targets by some small molecules and polyphenols to ameliorate diabetes-associated

Table 1
Effect of methyl-3β-hydroxylanosta-9, 24-dienoate (RA3), in the presence or absence of metformin (MET), on high glucose-mediated oxidative stress.

Prooxidants and Antioxidants	Treatment conditions					
	NG	NG + RA3	HG	RA3	MET	MET + RA3
ROS (RFU)	104.8 ± 8.03	95.3 ± 6.4	151.5 ± 9.2**	91.8 ± 4.9$^{\#\#\#}$	95.5 ± 5.6$^{\#\#\#}$	92.67 ± 5,0$^{\#\#\#}$
MDA (%)	100.2 ± 1.3	97.3 ± 1.2	143.7 ± 1.2***	122.3 ± 1.6$^{\#}$	121.0 ± 3.7$^{\#}$	111.2 ± 5.1$^{\#\#}$
GSH (RFU)	103 ± 3.4	115.3 ± 4.8	80.5V5.6*	118.5 ± 5.8$^{\#\#\#}$	112.1V4.2$^{\#\#\#}$	119.0 ± 7.2$^{\#\#\#}$
SOD (%)	100.0 ± 5.5	106.1 ± 2.0	30.7 ± 2.8***	74.19 ± 3.6$^{\#\#\#}$	64.2 ± 4.07$^{\#\#\#}$	82.8 ± 3.6$^{\#\#\#}$

Data are expressed as the mean ± SEM of 3 distinct biological experiments with each experiment having 3 technical replicates (n = 3). Significance is depicted as * $p \leq 0.05$, *** $p \leq 0.001$ *vs.* NG control, $^{\#}$ $p \leq 0.05$, $^{\#\#}$ $p \leq 0.01$, $^{\#\#\#}$ $p \leq 0.001$ *vs.* HG control. Abbreviations: ROS: reactive oxygen species; MDA: malondialdehyde; GSH: total glutathione content; SOD: superoxide dismutase; NG: normal glucose; HG: high glucose, RFU: relative fluorescence unit

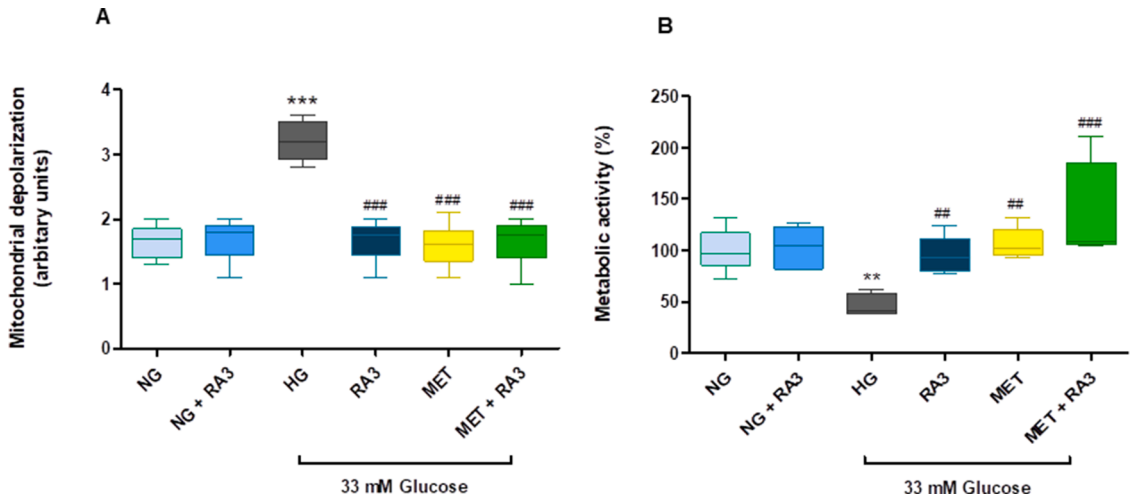

Fig. 4. The effect of methyl-3β-hydroxylanosta-9, 24-dienoate (RA3) and metformin (MET) on mitochondrial membrane potential and metabolic activity. (A) JC-1 fluorescence staining used to quantify mitochondrial depolarization and (B) ATP as a measurement of metabolic activity in high glucose (HG) stimulated H9c2 cells. Data are presented as the mean ± SEM of 3 separate biological experiments with each experiment having 3 technical repeats (n = 3). Significance is depicted as ** $p \leq 0.01$, *** $p \leq 0.001$ *vs.* NG control, ## $p \leq 0.01$ ### $p \leq 0.001$ *vs.* HG control.

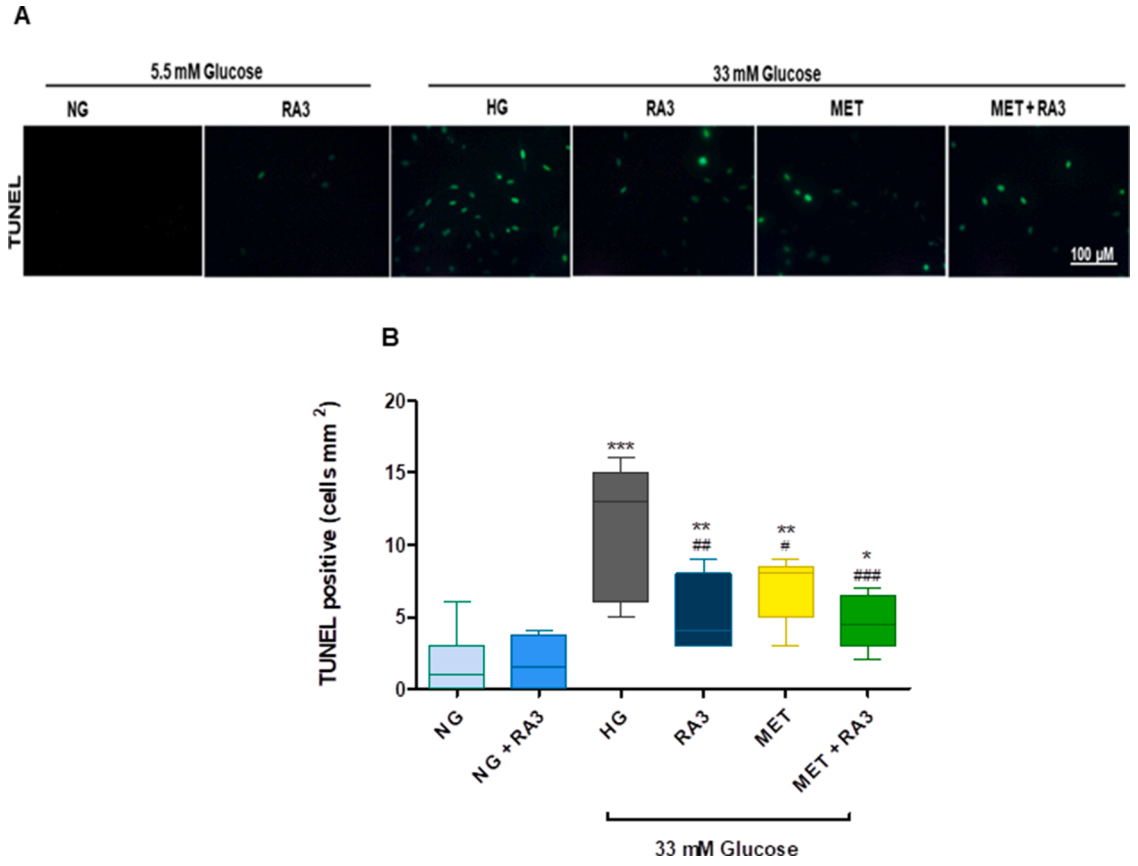

Fig. 5. Methyl-3β-hydroxylanosta-9, 24-dienoate (RA3), in the presence or absence of metformin (MET), attenuates high glucose-mediated DNA fragmentation. (A) Representative images of TUNEL fluorescence staining, and (B) quantification of TUNEL stained high glucose-stimulated H9c2 cells. Data is presented are expressed as the mean ± SEM of 3 separate biological experiments with each experiment having 3 technical repeats (n = 3). Significance is depicted as * $p \leq 0.05$, ** $p \leq 0.01$, *** $p \leq 0.001$ *vs.* NG control, # $p \leq 0.05$, ## $p \leq 0.01$ *vs.* HG control.

complications (Geraldes and King, 2010; Das et al., 2016).

Nonetheless, uncontrolled hyperglycemia, due to increased delivery of FFAs into the cardiomyocytes can activate PKC which contributes to peripheral insulin resistance by facilitating serine phosphorylation of IRS-1 (Hassan et al., 2016). Likewise, in the current study HG-stimulated cells presented with increased lipid content which led to the over-expression of PKC through the activation of diacylglycerol-PKC signal transduction pathway. Consequently, over-expression of PKC activated NF-κB in these cells, which is thought to function as a core effect in the cardiac hypertrophic response of DCM (Wang et al., 2009). In addition, phosphorylated PKC resulted in insulin signalling deregulation via the inhibition of the IRS-1/PI3K/Akt pathway. Evidently, the

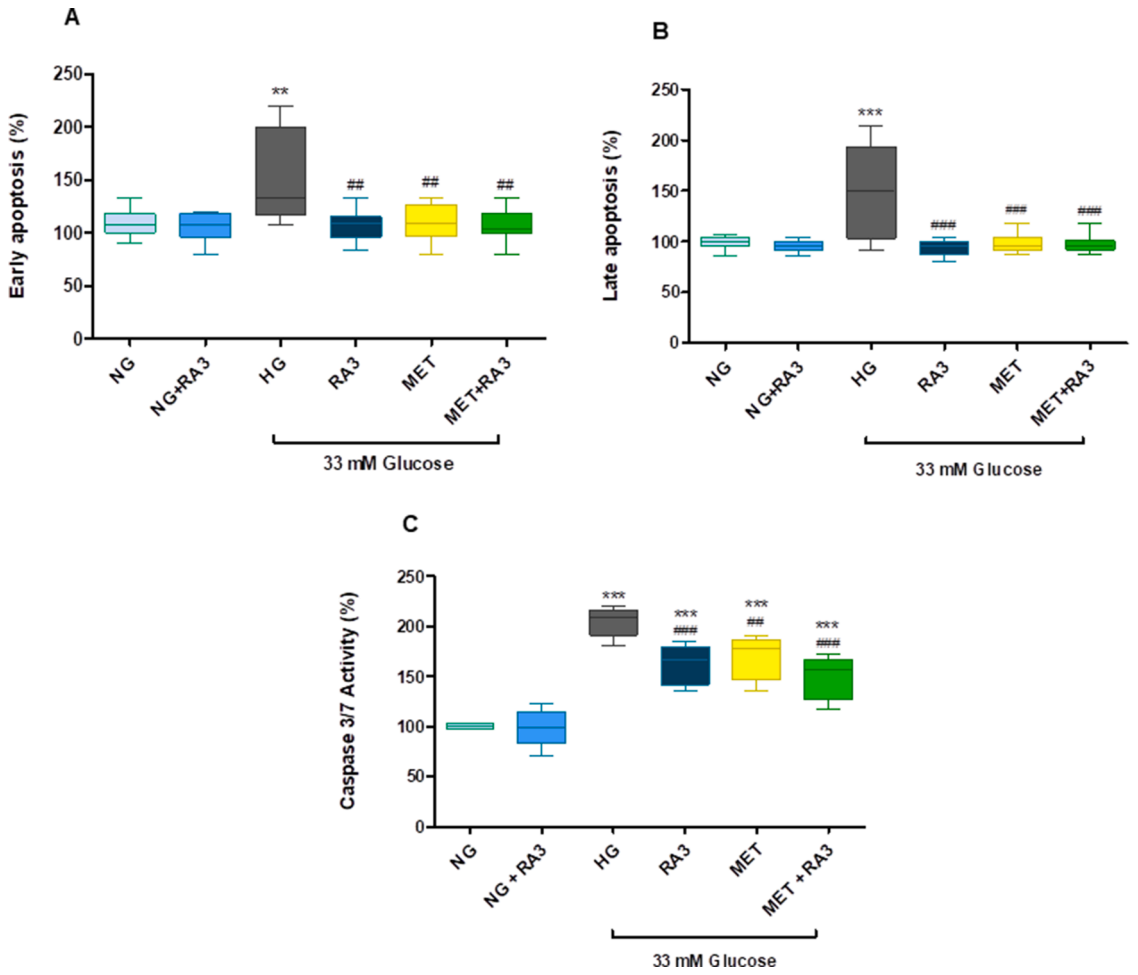

Fig. 6. Methyl-3β-hydroxylanosta-9, 24-dienoate (RA3), in the presence or absence of metformin (MET), mitigates high glucose-induced apoptosis. The rate of (A) early and (B) late apoptotic bodies as well as (C) caspase 3/7 activity in high glucose-stimulated H9c2 cells. Data is presented as the mean ± SEM of 3 separate biological experiments with each experiment having 3 practical repeats (n = 3). Significance is depicted as ** $p \leq 0.01$, *** $p \leq 0.001$ *vs*. NG control, ## $p \leq 0.01$, ### $p \leq 0.001$ *vs*. HG control.

optimal regulation of glucose transport is crucial to improve substrate metabolism in the diabetic heart. For example, previous reports have shown that the expression of GLUT4 is decreased in diabetic hearts which leads to a reduction in cardiac glucose influx in diabetic patients (Mishra et al., 2017; Szablewsk, 2017; Gu et al., 2018; Bowman et al., 2019). In this study, impaired insulin signalling reduced the expression of GLUT4 in HG-stimulated H9c2 cells, thus explaining the suppressed glucose uptake. Such results explain the increased screening of various pharmacological compounds for their protective effects against DCM by broadly targeting substrate metabolism, especially GLUT4 expression, in addition to other insulin signalling pathway markers such as PKC and PI3K/Akt so as to improve cellular glucose uptake.

Interestingly, we found that cardiomyoblasts treated with RA3 as a monotherapy or in combination with MET presented with improved glucose uptake and significantly reduced the levels of intracellular lipid content. These results were consistent with the triterpenes ability to improve substrate metabolism through enhanced insulin signalling under conditions of HG stress. As a result, RA3, with or without MET, alleviated the phosphorylation of the PKC-NF-κB cascade, whilst stimulating PI3K/Akt protein expression. While previous findings from our group have shown that RA3 improves the PI3K/Akt signalling pathway and enhances GLUT4 cytoplasmic translocation in skeletal muscles under diabetic conditions (Mabhida et al., 2018), the current results are the first to report the similar effects on the diabetic cardiomyoblast. Consistently, we observed an increased expression of pAMPK with RA3 treatment, which suggested an improvement in energy metabolism similar to insulin independent pathways. Beyond controlling insulin signalling, AMPK remains essential for regulating substrate metabolism by controlling the entry and oxidation of FFAs in the mitochondria, as previously discussed (Youssef et al., 2017; Cortassa et al., 2019). Thus, consistent with other naturally-derived compounds such as aspalathin or resveratrol (Johnson et al., 2016; Song et al., 2020), it appears that RA3 shows enhanced effects in protecting against DCM by effectively regulating energy metabolism, mainly through AMPK activation which is said to inhibit HG-induced oxidative stress and resultant cardiac oxidative damage (Hong et al., 2019). Of further interest was the ability of RA3 to enhance the efficacy of MET to ameliorate some of the measured parameters, like glucose uptake, which in turn attenuated the HG-mediated complications observed in our experimental model. These findings are indicative of a possible synergistic effect between RA3 and MET to improve cardiac efficiency under conditions of metabolic stress. However, further investigations, using *in vivo* experimental models, are required to explore this theory.

Accumulating evidence suggests that the accumulation of ROS and pro-oxidative stress products such as MDA, contributing to the expansion of infarct size and deterioration of cardiac function, play a critical role in diabetic cardiac injury (Kalogeris et al., 2014; Varga et al., 2015; Zhang et al., 2018). The prolonged effect of oxidative stress has the capacity to unduly exhaust endogenous antioxidants, such as SOD and GSH (Liao et al., 2017; Li et al., 2019). Notably, the results presented in

this study demonstrate that RA3, with or without MET, effectively attenuates HG-induced oxidative stress by restricting ROS production and lipid peroxidation. The triterpene also demonstrated an aptitude to enhance myocardial antioxidant enzyme (GSH and SOD) activity thus, offering additional protection against HG-induced oxidative stress. Such findings are in line with published literature showing that this triterpene displays strong antioxidant properties (Mosa et al., 2015; Mosa et al., 2016; Mabhida et al., 2018) which are important for its ameliorative effects against diabetes-linked complications. Scientific evidence also demonstrates that the combined use of polyphenol compounds with hypoglycaemic drugs are able to offer enhanced protection against diabetes-related cardiovascular complications and macrovascular dysfunction (Eriksson and Nyström, 2014; Wu et al., 2016).

According to literature antioxidant-based therapies, alone, have generally not been successful in diabetic patients (Lonn et al., 2005; Verma et al., 2017), suggesting that merely antagonizing existing ROS by enhancing endogenous antioxidant defence system may not be sufficient to abrogate DCM. Rather, a potentially more efficacious therapeutic approach might be to improve the overall capacity of mitochondrial quality control so as to preserve a pool of healthy mitochondria, which are needed for supporting cardiac contractile function in these patients (Verma et al., 2017). Likewise, in addition to its potent anti-oxidative properties, RA3 in the presence or absence of MET was able to ameliorate mitochondrial integrity and metabolic status, through the inhibition of HG-induced mitochondrial dysfunction. In accordance with this study's findings, Dludla and colleagues (2020) recently demonstrated that the combinational use of MET with a fermented rooibos extract can regulate cardiac mitochondrial energetics under hyperglycaemic conditions (Dludla et al., 2020). By improving MMP, we found that the apoptotic markers caspase 3/7 and DNA fragmentation were alleviated in HG-stimulated cells treated with RA3 or the combination of RA3 plus MET, which might have been attributed to the fact that intact mitochondrion rarely release cytochrome C (Grubb et al., 2001), which is actively involved in cell death pathways. In turn, the rate of early and late apoptosis was mitigated in these cells, suggesting that RA3 in the presence or absence of MET has an aptitude to effectively regulate apoptosis during periods of hyperglycemia. Such findings are rather important as accelerated cardiomyocyte loss is reported to reduce myocardial mass thereby, decreasing cardiac performance and ventricular dilatation (Chowdhry et al., 2007). These events are thought to be responsible for the relatively high mortality and morbidity rate in patients with DCM (Chowdhry et al., 2007). However, the results of this study suggest that such events could be alleviated through treatment with RA3 in combination with MET.

Conclusion

In the current study, we demonstrated for the first time that RA3 effectively alleviates HG-induced oxidative stress and mitochondrial dysfunction whilst reducing apoptosis in H9c2 cells. As an adjunct to MET, our findings confirmed that RA3 has an additive therapeutic potential on the anti-hyperglycemic effect of MET. This was demonstrated through enhanced cellular glucose uptake, antioxidant capacity and MMP. These findings suggest that RA3, as a monotherapy or supplement to MET, could potentially be an appropriate treatment against DCM. While this is indeed promising, a follow-up study using *in vivo* models should be conducted to further investigate the combined cardioprotective potential of RA3 with MET. Furthermore, the use of gene silencing techniques or inhibitors specific to the proposed regulatory pathway is needed to clearly understand the exact mechanism by which RA3 offers its cardioprotection. As such, the former as well as the expression of GLUT4 in the plasma membrane and the total expression of the proteins (AMPK, NF-κB, IRS,PKC and Akt) involved in insulin dependent and independent signaling should be investigated in a follow-up, as these were some of the limitations to the current study.

CRediT author statement

Nonhlakanipho F. Sangweni: Conceptualization, Methodology, Formal analysis, Investigation, Writing - Original draft, Writing - review & editing, Visualization, Project administration. Rebamang A. Mosa: Conceptualization, Methodology, Resources, Supervision, Writing - review & editing, Project administration. Phiwayinkosi V. Dludla: Conceptualization, Methodology, Formal analysis, Writing - review & editing. Abidemi P. Kappo: Writing - review & editing, Supervision, Funding acquisition. Andy R. Opoku: Conceptualization. Christo J.F Muller: Supervision. Rabia Johnson: Conceptualization, Methodology, Resources, Supervision, Writing - review & editing, Project administration, funding acquisition.

Funding

The work reported herein was made possible through funding by the South African Medical Research Council (SAMRC) through its Division of Research Capacity Development under the Internship Scholarship Programme and Research Strengthening and Capacity Development Funding Opportunity for Selected Universities Initiative (Grant No. PC 57009). The content hereof is the sole responsibility of the authors and does not necessarily represent the official views of the SAMRC. The authors would also like to acknowledge the financial support from the SAMRC, Biomedical Research and Innovation Platform (baseline funding) and SAMRCs Intra-Mural Postdoctoral Fellowship Programme through which funding received from the South African National Treasury. Lastly, we would also like to acknowledge the National Research Foundation for the financial support (Thuthuka Grant (UID120812))

Declaration of Competing Interest

The authors declare that there are no conflicts of interests.

Acknowledgments

The findings reported in this manuscript were supported by the SAMRC through funding received from the South African National Treasury. We would also like to acknowledge the Biomedical Research and Innovation Platform.

References

Borghetti, G., von Lewinski, D., Eaton, D.M., Sourij, H., Houser, S.R., Wallner, M., 2018. Diabetic cardiomyopathy: current and future therapies. Beyond Glycemic Control. Front. Psychol. 9, 1514.

Bowman, P.R.T., Smith, G.L., Gould, G.W., 2019. GLUT4 expression and glucose transport in human induced pluripotent stem cell-derived cardiomyocytes. PLoS ONE 14 (7), e0217885.

Bugger, H., Abel, E.D., 2010. Mitochondria in the diabetic heart. Cardiovasc. Res. 88 (2), 229–240.

Chowdhry, M.F., Vohra, H.A., Galiñanes, M., 2007. Diabetes increases apoptosis and necrosis in both ischemic and nonischemic human myocardium: role of caspases and poly–adenosine diphosphate–ribose polymerase. J. Thorac. Cardiovasc. Surg. 134 (1), 124–131.

Cortassa, S., Aon, M.A., Sollott, S.J., 2019. Control and regulation of substrate selection in cytoplasmic and mitochondrial catabolic networks. a systems biology analysis. Front. Psychol. 10, 201.

Das, J., Ramani, R., Suraju, M.O., 2016. Polyphenol Compounds and PKC Signaling. Biochim. Biophys. Acta, Gen. Subj. 1860 (10), 2107–2121.

Davargaon, R.S., Sambe, A.D., Muthangi, S., 2018. Toxic effect of high glucose on cardiomyocytes, H9c2 cells: Induction of oxidative stress and ameliorative effect of trolox. J. Biochem. Mol. Toxicol. 33 (4), e22272.

De Rosa, S., Arcidiacono, B., Chiefari, E., Brunetti, A., Indolfi, C., Foti, D.P., 2018. Type 2 Diabetes mellitus and cardiovascular disease: genetic and epigenetic. Front. Endocrinol. 9, 2.

Dludla, P.V., Gabuza, K.B., Muller, C.J.F., Joubert, E., Louw, J., Johnson, R., 2018. Aspalathin, a C-glucosyl Dihydrochalcone from rooibos improves the hypoglycemic potential of metformin in type 2 Diabetic (db/db) Mice. Physiol. Res. 67, 813–818.

Dludla, P.V., Johnson, R., Mazibuko-Mbeje, S., Muller, C.J.F., Louw, J., Joubert, E., Orlando, P., Silvestri, S., Chellan, N., Nkambule, B., Essop, F., Tiano, L., 2020. Fermented rooibos extract attenuates hyperglycemia-induced myocardial oxidative

damage by improving mitochondrial energetics and intracellular antioxidant capacity. S. Afr. J. Bot. 131, 143–150.
Eriksson, L., Nyström, T., 2014. Activation of AMP-activated protein kinase by metformin protects human coronary artery endothelial cells against diabetic lipoapoptosis. Cardiovasc Diabetol 13, 152.
Gawli, K., Lakshmidevi, N., 2015. Antidiabetic and antioxidant potency evaluation of different fractions obtained from Cucumis prophetarum fruit. Pharm Biol 689–694.
Geraldes, P., King, G.L., 2010. Activation of Protein Kinase C Isoforms & its impact on diabetic complications. Circ. Res. 106 (8), 1319–1331.
Grubb, D.R., Ly, J.D., Vaillant, F., Johnson, K.L., Lawen, A., 2001. Mitochondrial cytochrome c release is caspase-dependent and does not involve mitochondrial permeability transition in didemnin B-induced apoptosis. Oncogene 20, 4085–4094.
Gu, J., Wang, S., Guo, H., Tan, Y., Liang, Y., Feng, A., Liu, Q., Damodaran, C., Zhang, Z., Keller, B.B., Zhang, C., Cai, L., 2018. Inhibition of p53 prevents diabetic cardiomyopathy by preventing early-stage apoptosis and cell senescence, reduced glycolysis, and impaired angiogenesis. Cell Death Dis 9, 82.
Hajar, R., 2017. Diabetes as "Coronary Artery Disease Risk Equivalent": a historical perspective. heart views 18 (1), 34–37.
Hassan, R.H., Pacheco de Sousa, A.C., Mahfouz, R., Hainault, I., Blachnio-Zabielska, A., Bourron, O., Koskas, F., Górski, J., Ferré, P., Foufelle, F., Hajduch, E., 2016. Sustained action of ceramide on the insulin signaling pathway in muscle cells implication of the double-stranded RNA-Activated Protein Kinase. J. Biol. Chem. 291 (6), 3019–3029.
Hong, S., Hwang, H., Kim, J.W., Kim, J.A., Lee, Y.B., Roh, E., Choi, SK.M., Baik, S.H., Yoo, H.J., 2019. Ginsenoside compound-Mc1 attenuates oxidative stress and apoptosis in cardiomyocytes through an AMP-activated protein kinase–dependent mechanism. J Ginseng Res 1226–8453.
Isfort, M., Stevens, S.C.W., Schaffer, S., Jong, C.J., Wold, L.E., 2014. Metabolic dysfunction in diabetic cardiomyopathy. Heart Fail. Rev. 19, 35–48.
Jia, G., Hill, M.A., Sowers, J.R., 2018. Diabetic cardiomyopathy: an update of mechanisms contributing to this clinical entity. Circ. Res. 122 (4), 624–638.
Johnson, R., Dludla, P., Joubert, E., February, F., Mazibuko, S., Ghoor, S., Muller, C., Louw, J., 2016. Aspalathin, a dihydrochalcone C -glucoside, protects H9c2 cardiomyocytes against high glucose induced shifts in substrate preference and apoptosis. Mol. Nutr. Food Res. 60 (4), 922–934.
Kalogeris, T., Bao, Y., Korthuis, R.J., 2014. Mitochondrial reactive oxygen species: a double edged sword in ischemia/reperfusion vs. preconditioning. Redox Biol 2, 702–714.
Li, K., Zhai, M., Jiang, L., Song, F., Zhang, B., Li, J., Li, H., Li, B., Xia, L., Xu, L., Cao, Y., He, M., 2019. Tetrahydrocurcumin ameliorates diabetic cardiomyopathy by attenuating high glucose-induced oxidative stress and fibrosis via activating the SIRT1 Pathway. Oxid. Med. Cell. Longev. 6746907, 15.
Liao, H., Zhu, J., Feng, H., Ni, J., Zhang, N., Chen, S., Liu, H., Yang, Z., Deng, W., Tang, Q., 2017. Myricetin Possesses potential protective effects on diabetic cardiomyopathy through inhibiting IκBα/NFκB and enhancing Nrf2/HO-1. Oxid. Med. Cell. Longev. 8370593, 14.
Lonn, E., Bosch, J., Yusuf, S., Sheridan, P., Pogue, J., Arnold, J.M., Ross, C., Arnold, A., Sleight, P., Probstfield, J., Dagenais, G.R., Hope, H.T.T., 2005. Effects of long-term vitamin E supplementation on cardiovascular events and cancer: a randomized controlled trial. J. Am. Med. Assoc. 293, 1338–1347.
Luo, B., Li, B., Wang, W., Liu, X., Xia, Y., Zhang, C., Zhang, M., Zhang, Y., An, F., 2014. NLRP3 Gene silencing ameliorates diabetic cardiomyopathy in a Type 2 Diabetes Rat Model. PLoS One 9 (8), e104771.
Mabhida, S.E., Johnson, R., Ndlovu, M., Sangweni, N.F., Johan, J., Opoku, A., Mosa, R. A., 2018. A Lanosteryl triterpene from Protorhus longifolia augments insulin signaling in type 1 diabetic rats. BMC Complement Altern. Med. 18, 265.
Machaba, K.E., Cobongela, S.Z.Z., Mosa, R.A., Lawal, O.A., Djarova, T.G., Opoku, A.R., 2014. *In vivo* anti-hyperlipidemic activity of the triterpene from the stem bark of Protorhus longifolia (Benrh) Engl. Lipids Health Dis 13, 131.
Makarova, E., Makrecka-Kuka, M., Vilks, K., Volska, K., Sevostjanovs, E., Grinberga, S., Zarkova-Malkova, O., Dambrova, M., Liepinsh, E., 2019. Decreases in circulating concentrations of long-chain acylcarnitines and free fatty acids during the glucose tolerance test represent tissue-specific insulin sensitivity. Front. Endocrinol. 10, 870.
Marcinkiewicz, A., Ostrowski, S., Drzewoski, J., 2017. Can the onset of heart failure be delayed by treating diabetic cardiomyopathy. Diabetol. Metab. Syndr. 9, 21.
Mishra, P.K., Ying, W., Nandi, S.S., Bandyopadhyay, G.K., Patel, K.K., Mahata, S.K., 2017. Diabetic Cardiomyopathy: an Immunometabolic Perspective. Front. Endocrinol. 8, 72.
Mosa, R.A., Cele, N.D., Mabhida, S.E., Shabalala, S.C., Penduka, D., Opoku, A.R., 2015. *In Vivo* Antihyperglycemic activity of a Lanosteryl Triterpene from Protorhus longifolia. Molecules 20, 13374–13383.
Mosa, R.A., Hlophe, N.B., Ngema, N.T., Penduka, D., Lawal, O.A., Opoku, A.R., 2016. Cardioprotective Potential of a Lanosteryl Triterpene from Protorhus longifolia. Pharm. Biol. 54 (12), 3244–3248.
Mosa, R.A., Naidoo, J.J., Nkomo, F.S., Mazibuko, S.E., Muller, C.J., Opoku, A.R., 2014. *In vitro* antihyperlipidemic potential of triterpenes from stem bark of Protorhus longifolia. Planta Med 80, 1685–1691.
Naruszewiczac, M., Łaniewskab, I., Milloc, B., Dłużniewski, M., 2007. Combination therapy of statin with flavonoids rich extract from chokeberry fruits enhanced reduction in cardiovascular risk markers in patients after myocardial infraction (MI). Atherosclerosis 194 (2), 179–184.
Ormazabal, V., Nair, S., Elfeky, O., Aguayo, C., Salomon, C., Zuñiga, F.A., 2018. Association between insulin resistance and the development of cardiovascular disease. Cardiovasc Diabetol 17, 122.
Rahimi, G., Heydari, S., Rahimi, B. et al. A combination of herbal compound (SPTC) along with exercise or metformin more efficiently alleviated diabetic complications through down-regulation of stress oxidative pathway upon activating Nrf2-Keap1 axis in AGE rich diet-induced type 2 diabetic mice. Nutr Metab., 18, 14.
Rider, O.J., Cox, P., Tyler, D., Clarke, K., S Neubauer, S., 2013. Myocardial substrate metabolism in obesity. Int J Obes 37, 972–979.
Rubler, S., Dlugash, J., Yuceoglu, Y.Z., Kumral, T., Branwood, A.W., Grishman, A., 1972. New type of cardiomyopathy associated with diabetic glomerulosclerosis. Am J Cardiol 30, 595–602.
Sangweni, N.F., Dludla, P.V., Mosa, R.A., Kappo, A.P., Opoku, A., Muller, C.J.F., Johnson, R., 2018. Lanosteryl triterpenes from Protorhus longifolia as a cardioprotective agent: a mini review. Heart Fail Rev 1382–4147.
Song, Y.J., Zhong, C.B., Wu, W., 2020. Oxid. Med. Cell. Longev., 7051845
Sun, S., Yang, S., Dai, M., Jia, X., Wang, Q., Zhang, Z., Mao, Y., 2017. The effect of Astragalus polysaccharides on attenuation of diabetic cardiomyopathy through inhibiting the extrinsic and intrinsic apoptotic pathways in high glucose -stimulated H9C2 cells. BMC Complement Altern. Med. 17, 310.
Suryavanshi, S.V., Kulkarni, Y.A., 2017. NF-κβ: A Potential Target in the Management of Vascular Complications of Diabetes. Front Pharmacol 7 (8), 798.
Szablewsk, L., 2017. Glucose transporters in healthy heart and in cardiac disease. Int. J. Cardiol. 230, 70–75.
Tate, M., Grieve, D.J., Ritchie, R.H., 2017. Are targeted therapies for diabetic cardiomyopathy on the horizon. Clin Sci 131 (10), 897–915.
Varga, Z.V., Giricz, Z., Liaudet, L, Haskó, G., Ferdinandy, P., Pacher, P., 2015. Interplay of oxidative, nitrosative/nitrative stress, inflammation, cell death and autophagy in diabetic cardiomyopathy. Biochim. Biophys. Acta. 1852 (2), 232–242.
Verma, S.K., Garikipatia, V.N.S., Kishore, R., 2017. Mitochondrial dysfunction and its impact on diabetic heart. Biochim Biophys Acta Mol Basis Dis 1863 (5), 1098–1105.
Wang, M., Zhang, W.B., Zhou, B.Q., Zhu, J.H., Fu, G.S., 2009. The signal transduction pathway of PKC/NF-κB/c-fos may be involved in the influence of high glucose on the cardiomyocytes of neonatal rats. BMC Cardiovasc Diabetol 8, 8.
Wu, P., Yu Yan, Y., Ma, L., Hou, B., He, Y., Zhang, L., Niu, Z., Song, J., Pang, X., Yang, X., Du, G., 2016. Effects of the Nrf2 Protein Modulator Salvianolic Acid A alone or combined with metformin on diabetes-associated macrovascular and renal injury. J. Biol. Chem. 291 (42), 22230–22288.
Youssef, N., Campbell, S., Barr, A., Gandhi, M., Hunter, B., Dolinsky, V., Dyck, J.R.B., Clanachan, A.S., Peter, E., Light, P.E., 2017. Hearts lacking plasma membrane KATP channels display changes in basal aerobic metabolic substrate preference and AMPK activity. Am J Physiol Heart Circ Physiol 313, H469–H478.
Zhang, B., Zhai, M., Li, B., Liu, Z., Li, K., Jiang, L., Zhang, M., Yi, W., Yang, J., Yi, D., Liang, H., Jin, Z., Duan, W., Shiqiang, Y., 2018. Honokiol Ameliorates Myocardial Ischemia/Reperfusion Injury in Type 1 Diabetic rats by reducing oxidative stress and apoptosis through activating the SIRT1-Nrf2 signaling pathway. Oxid. Med. Cell. Longev., 3159801
Zhao, C., Zhang, Y., Liu, H., Li, P., Zhang, H., Cheng, G., 2017. Fortunellin protects against high fructose-induced diabetic heart injury in mice by suppressing inflammation and oxidative stress via AMPK/Nrf-2 pathway regulation. Biochem. Biophys. Res. Commun. 490 (2), 552–559.